Phase Inversion on Sieve Trays

W. VAL PINCZEWSKI, NEILL D. BENKE, and CHRISTOPHER J. D. FELL

School of Chemical Engineering, University of New South Wales, Australia

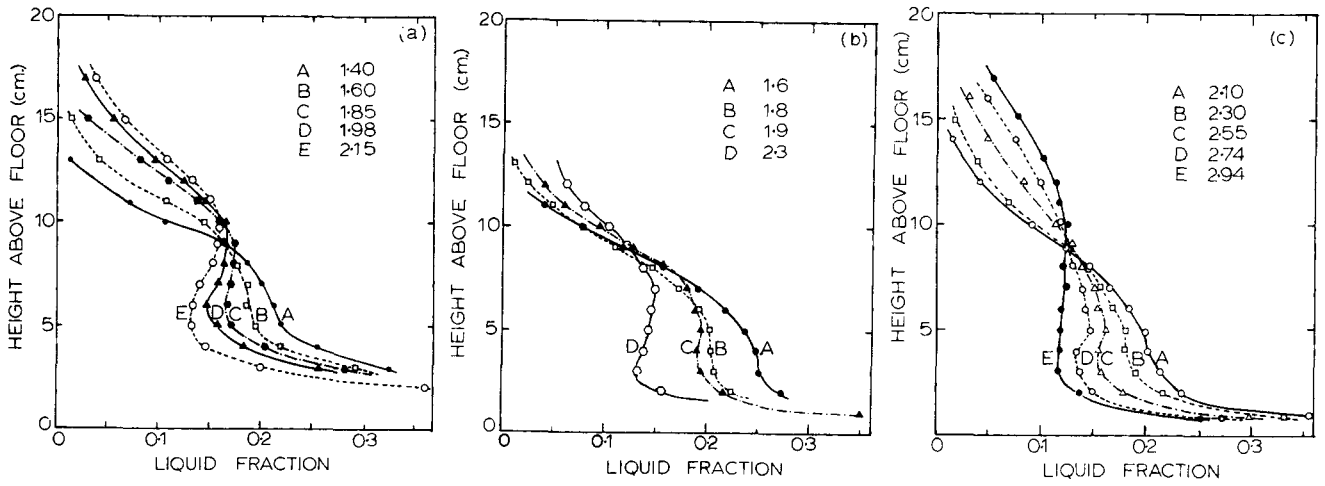

Fig. 1. Vertical dispersion density profiles for 1.27 cm (½ inch) hole diameter trays of three free areas. Liquid cross flow: 19 m^3/hr-m-weir. Values given on curves are gas loadings expressed as F_S ms^{-1} $(kg/m^3)^{1/2}$. Phase inversion loadings for these trays are:

	% Free Area	F_S at Inversion ms^{-1} $(kg/m^3)^{1/2}$
(a)	5.9	1.85
(b)	10.4	2.20
(c)	16.1	2.55

Phase inversion on a sieve tray contactor occurs when the gas loading is sufficiently high for the dispersion on the tray to change from predominantly a froth (liquid continuous) to a spray (gas continuous). Methods are now available (Porter and Wong, 1969; Loon et al., 1973; Jeronimo and Sawistowski, 1973) for predicting the gas loading at which phase inversion will occur. Porter and Lockett (1975) have shown that these may be applied to industrial scale columns and have suggested that many such columns are operated in a stable spray regime. When experimental sieve tray performance data in the literature (Hunt et al., 1955; McAllister et al., 1958; Friend et al., 1960; Barker and Self, 1962; Lemieux and Scotti, 1969) are similarly examined, it is found that investigators have not infrequently unknowingly operated their trays beyond the point of phase inversion. Yet, all available correlations for sieve tray parameters, such as pressure drop and entrainment, are based on the premise that the dispersion is a froth.

It is therefore of interest to examine more closely the impact of phase inversion on tray hydrodynamic behavior. To this end, this note reports detailed experimental measurements taken on simulated industrial sieve trays at loadings spanning the phenomenon of inversion. The results are for large hole diameter trays characteristic of those in industrial service.

EXPERIMENTAL

The experimental measurements were made on an air-water simulator having an active area of 0.61 × 0.31 m and able to be operated at high gas and liquid loadings. The unit (Pinczewski and Fell, 1972) was designed to duplicate hydrodynamic conditions at the center section of an industrial scale sieve tray. Three types of measurements were taken: vertical dispersion density profiles, tray pressure drop, and tray entrainment, all for 1.27 cm (½ in.) hole diameter trays having free areas of 5.9, 10.7, and 16.1%, respectively. Vertical dispersion density profiles were determined by gamma ray attenuation (Pinczewski and Fell, 1974). Pressure drop was measured by an inclined U tube manometer. Free entrainment as reported consisted of all liquid collected by a baffle type of deentrainment device fitted 0.91 m above the tray floor. Gas velocities at phase inversion used in interpreting results obtained have been taken from Loon et al., (1973). In all runs a weir height of 2.5 cm was used.

Correspondence concerning this note should be sent to Christopher J. D. Fell, Chemical Engineering Department, University of Illinois, Urbana, Illinois 61801. W. Val Pinczewski is with Esso Australia, Ltd., Sydney, Australia.

EFFECT OF INVERSION ON THE DISPERSION

Vertical dispersion density profiles at various gas loadings are shown in Figures 1*a* to *c*. The profiles in the fully developed spray regime complement those reported earlier by the present authors (1974) for slightly lower liquid loadings. For all three trays, which cover the range of free areas in industrial application, the profiles show that the nature of the dispersion on the tray undergoes an orderly change as the gas loading is increased. At low superficial F factors [$F_S = U_S \sqrt{\rho_g}$ ms^{-1} $(kg/m^3)^{1/2}$], the profiles are consistent with the bulk of the dispersion, being in the form of the classic froth on which tray correlations are modeled. Beyond the point of phase inversion the profiles suggest that the dispersion is in the form of a coarse spray. The cause and significance of the observed maximum in the dispersion density profile in this regime have been previously discussed (Pinczewski and Fell, 1974). It it noteworthy that the dispersion density profiles obtained on the present industrial scale trays closely follow the shape above and below phase inversion described by Fane and Sawistowski (1969) for actual distillation conditions on a 0.11 × 0.19 m tray with 0.3 cm holes. The shape of the dis-

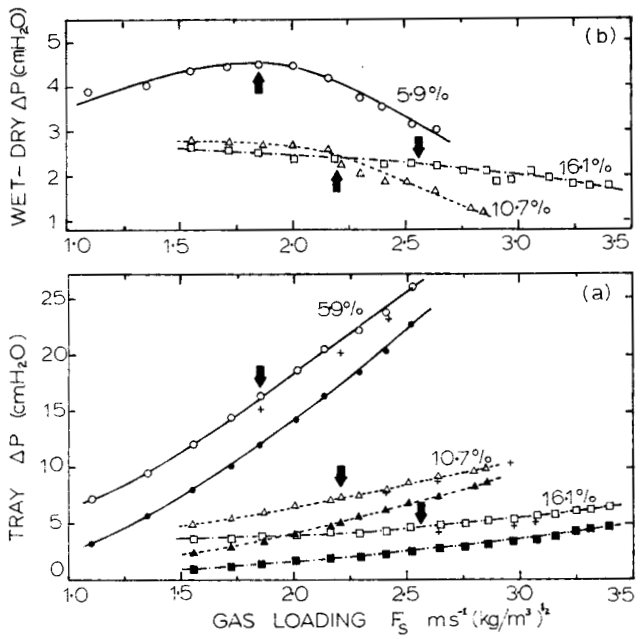

Fig. 2. Pressure drop for three trays studied. Lower curve for each tray in Fig. 2(a) is dry tray pressure drop. Difference between wet and dry tray pressure drops plotted on Fig 2b. + on Figure 2a represents equivalent pressure drop obtained by adding liquid holdup from integration of vertical dispersion density profile to dry tray pressure drop. All results are for a liquid cross flow of 15 m³/hr-m-weir. Points of phase inversion are arrowed.

persion density profile thus appears generally indicative of the regime of tray operation, irrespective of specific tray geometry, an observation that can perhaps be applied to the on-line study of industrial tray performance.

EFFECT OF INVERSION ON TRAY PRESSURE DROP

Figures 2*a* and *b* give typical pressure drop data for the trays studied. Tray total pressure drop (Figure 2*a*) is strongly influenced by tray free area and is seen to increase steadily with gas loading up to and beyond the point of phase inversion. Reported wet tray pressure drops for the 10.7% free area tray agree with earlier values (Lemieux and Scotti, 1969). The effect of phase inversion on tray pressure drop can be most readily seen from Figure 2*b*. For each tray the difference between wet and dry pressure drops becomes less with increasing gas velocity beyond phase inversion. This cannot be explained in terms of decrease in tray liquid holdup as is done in the froth regime, as integration of the vertical dispersion density profiles reveals that liquid holdup, though decreasing with increased gas loading in the spray regime (Pinczewski and Fell, 1974), does not decrease at a sufficient rate to explain the discrepancy. It would therefore appear that a different mechanism is responsible for the nondry tray component of total pressure drop when the tray is operating in the spray regime. This is not surprising, as the gas leaving the

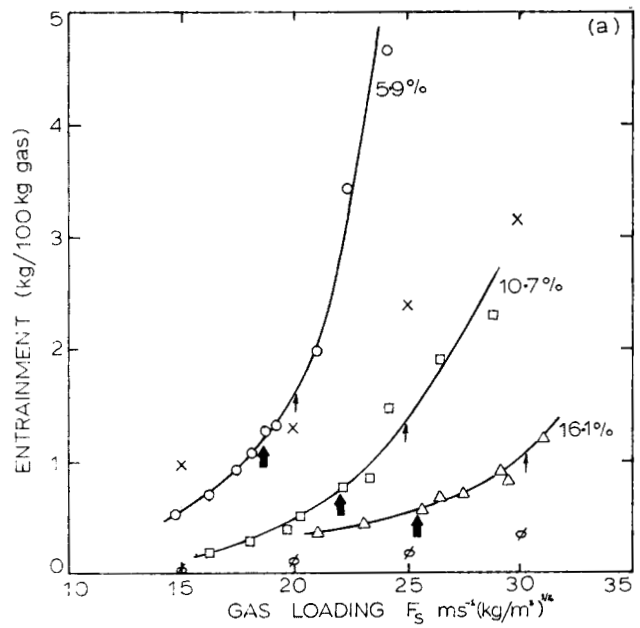

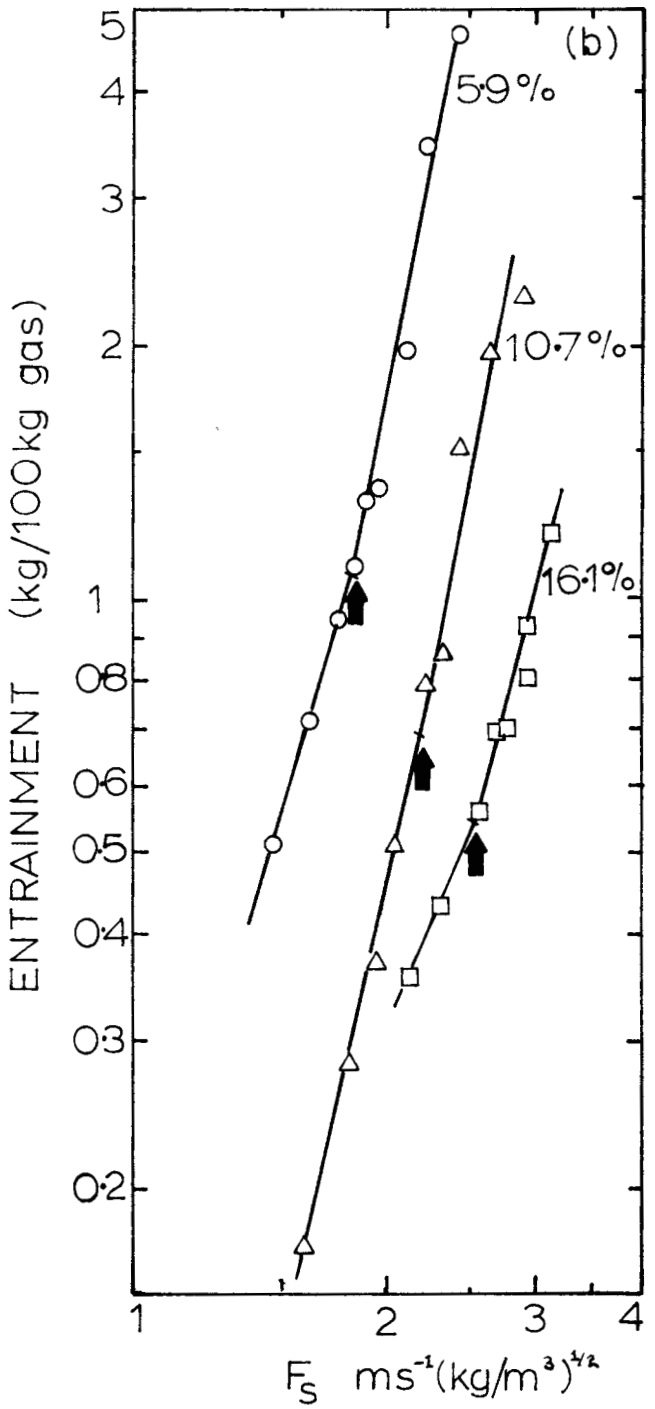

Fig. 3. Entrainment collected 0.91 m above tray floor for three trays studied. Figure 3(b) is plotted in logarithmic co-ordinates. X and ϕ represent predicted values from equations of Fair (1973) and Hunt et al., (1955), respectively. All results are for a liquid cross flow of 15 m³/hr-m-weir. Points of phase inversion are heavily arrowed. Light arrows show points where entrainment reaches 25 lb/hr-ft² tray area.

tray orifices no longer encounters continuous liquid as in the froth regime. As yet, however, there is no method available for predicting the pressure drop associated with the pulsating gas flume that is formed at each orifice.

One further observation from Figure 2*a* is that the dry tray pressure drop measurements are not well predicted by available correlations. In view of the dominance of dry tray pressure drop in overall pressure drop in the spray regime, this represents a serious shortcoming of existing correlations for tray design. The equations of McAllister et al. (1958) and Fair (1973) overpredict by an average of 22 and 35%, respectively. That of Hunt et al. (1955) underpredicts by an average of 15%. The best fit for all reported data (average mean-square error 7%) is obtained by adopting the form of Hunt's equations as in Equation (1), with the constant C set at 1.30:

$$h_d = 100\,C\,\frac{\rho_g}{\rho_l}\,\frac{U_h^2}{2g}\,[0.4(1.25 - A_F) + (1 - A_F)^2] \qquad (1)$$

EFFECT OF INVERSION ON ENTRAINMENT

Entrainment data for the three trays studied are given in Figures 3*a* and *b*. The values reported have been measured sufficiently far above the tray floor to be no longer influenced by droplets properly belonging to the dispersion but undergoing an extended vertical trajectory. This is an important consideration in the spray regime, where the upper boundary of the dispersion can no longer be defined. The reported entrainments can be interpreted as a measure of the quantity of those droplets having terminal velocities lower than the column superficial velocity.

The data on Figure 3*a* show that entrainment is strongly influenced by hole free area, with entrainment being greatest from the lowest free area tray. This dependence is not accounted for by plotting the results in terms of hole F factors [$U_h \sqrt{\rho_g}$ ms^{-1}(kg/m^3)$^{1/2}$]. For each tray studied, the entrainment is seen to increase rapidly with increasing gas loading up to and beyond phase inversion. From Figure 3*b* it can be seen that beyond the point of phase inversion the dependence of entrainment on gas loading changes. A similar observation may be made for the entrainment data reported by Hunt et al. (1955, their Figures 8 and 9). Such a change in dependence of entrainment on gas loading at phase inversion is not unexpected, as the mechanism by which the entrainment droplet population is produced passes from one of bubble film rupture in the froth regime to one of jet atomization in the spray regime. However, the new dependence in the spray regime depends further on tray free area, suggesting a mechanism more complex than one accounting for hole velocity alone.

The present entrainment data have been compared with predictions from the correlations of Hunt et al. (1955) and Fair (1973). The former correlation, which does not account for free area and is based on froth regime data, severely underpredicts the present results. The latter correlation, which does account for free area effects through percentage approach to flooding, gives predictions in reasonable agreement with experiment at low loadings but severely overpredicts entrainment from high free area trays operating in the spray regime. Comparison of the present data with the experimental entrainment data of Friend et al. (1960) and Lemieux and Scotti (1969) on similar hole diameter trays is not possible, as these authors have measured entrainment much closer to the tray floor. In the spray regime they have observed very large entrainments, but this can be attributed to collection of droplets having quite large terminal velocities on the upward part of their trajectories. From Figures 1*a* to *c* and previous work of the present authors (1974), the dispersion zone is found to extend to a height of 30 cm or more above the tray floor in the fully developed spray regime.

DISCUSSION

The experimental information presented is representative of extensive measurements made on a series of trays having hole diameters of 0.64 to 1.91 cm (¼ to ¾ in.) and free areas of 5 to 15% at industrial loadings (Pinczewski, 1972; Benke, 1974). For all trays studied, the results obtained were the same, independent of tray geometry; the vertical dispersion density profile changed its shape past phase inversion, and entrainment and the nondry tray component of pressure drop showed a somewhat different dependence on gas loading in the spray regime than in the froth regime.

Thus, while there is no dramatic change apparent in tray hydrodynamic parameters such as pressure drop and entrainment at the point of phase inversion itself, it is seen that hydrodynamic behavior of the tray alters as the tray enters the spray regime. Clearly, this new regime needs to be modeled in a different way than is customary for the froth regime. At present, the orifice atomization processes determining spray regime behavior are not fully understood. However, it is suggested that this may be an important area for further study if adequate prediction methods for sieve tray spray regime operating parameters are to be developed.

NOTATION

A_F = fractional tray free area based on active or bubbling area
C = constant in Equation (1)
F_h = hole F factor [$U_h \sqrt{\rho_g}$ ms^{-1} (kg/m^3)$^{1/2}$]
F_S = superficial F factor [$U_S \sqrt{\rho_g}$ ms^{-1} (kg/m^3)$^{1/2}$]
g = gravitational acceleration, ms^{-2}
h_d = dry tray pressure drop, cm liquid
U_h = hole velocity, ms^{-1}
U_S = column superficial velocity, ms^{-1}
ρ_g = gas density, kg/m^3
ρ_l = liquid density, kg/m^3

LITERATURE CITED

Barker, P. E., and M. F. Self, "The Evaluation of Liquid Mixing Effects on a Sieve Plate Using Unsteady and Steady State Tracer Techniques," *Chem. Eng. Sci.*, **17**, 541 (1962).

Benke, N. D., B. E. thesis, Univ. of New South Wales, Australia (1974).

Fair, J. R., in *Chemical Engineers' Handbook*, R. H. Perry and C. H. Chilton, ed., pp. 18-6-18-13, McGraw Hill, New York (1973).

Fane, A. G. and H. Sawistowski, "Plate Efficiencies in the Foam and Spray Regimes of Sieve-Plate *Distillation, 1969* (London: Inst. Chem. Engrs.), **1**, 8 (1969).

Friend, L., E. J. Lemieux, and W. C. Schreiner, "New Data on Entrainment from Perforated Trays at Close Spacings," *Chem. Eng.*, **101**, (October 31, 1960).

Hunt, C. d'A., D. N. Hanson, and C. R. Wilke, "Capacity Factors in the Performance of Perforated-Plate Columns," *AIChE J.*, **1**, 441 (1955).

Jeronimo, M. A. da S., and H. Sawistowski, "Plate Inversion Correlation for Sieve Trays," *Trans. Inst. Chem. Engrs.*, **51**, 265 (1973).

Lemieux, E. J., and L. J. Scotti, "Perforated Tray Performance," *Chem. Eng. Progr.*, **65**, No. 3, 52 (1969).

Loon, R. E., W. V. Pinczewski, and C. J. D. Fell, "Dependence of the Froth-to-Spray Spray Transition on Sieve Tray Design Parameters," *Trans. Inst. Chem. Engrs.*, **51**, 374 (1973).

McAllister, R. A., P. H. McGinnis, Jr., and C. A. Plank, "Perforated Plate Performance," *Chem. Eng. Sci.*, **9**, 25 (1958).

Pinczewski, W. V., Ph.D. thesis, Univ. of New South Wales, Australia (1973).
———, and C. J. D. Fell, "The Transition from Froth-to-Spray Regime on Commercially Loaded Sieve Trays," *Trans. Inst. Chem. Engrs.*, **50**, 102 (1972).
———, "Nature of the Two-Phase Dispersion on Sieve Plates Operating in the Spray Regime," *ibid.*, **52**, 294 (1974).
Porter, K. E., and M. J. Lockett, "Prediction of Plate Efficiency in Columns of Large Diameter," Paper presented at AIChE National Meeting, Houston, Tex. (1975).
Porter, K. E., and P. F. Y. Wong, "Transition from Spray to Bubbling on Sieve Trays," *Distillation, 1969* (London: Inst. Chem. Engrs.), **2**, 22 (1969).

Manuscript received July 7, 1975; revision received September 16 and accepted September 18, 1975.

Some Liquid Holdup Experimental Data in Trickle-Bed Reactors for Foaming and Nonfoaming Hydrocarbons

JEAN-CLAUDE CHARPENTIER and MICHEL FAVIER

Laboratoire des Sciences du Génie Chimique, CNRS
Ecole Nationale Superieure des Industries Chimiques—54042 NANCY CEDEX (France)

TABLE 1. PACKING PROPERTIES

Type	Glass spheres	Spherical catalyst	Cylindrical catalyst 1	Cylindrical catalyst 2
d, mm	3	3	1.8 × 6	1.4 × 5
ϵ, external void	0.38	0.39	0.39	0.37
a_g, m^{-1}	2,000	2,000	2,555	3,257
β_c	0.10	0.077-0.11	0.08	0.06-0.08
D, m	0.10	0.05	0.05	0.05
h_k	12.5	5.75-5.66	4	3.5
h_B	0.274	0.303-0.40	0.515	0.28

From the recent and excellent review paper written by Satterfield (1975), it appears that authors disagree on the use of predicting correlations for liquid holdup in trickle-bed reactors (Satterfield and Way, 1972; Henry and Gilbert, 1973; Mears, 1974; Wijffels et al., 1974). For this fundamental parameter for the design of such reactors, we would like to present experimental data concerning twenty gas-hydrocarbons systems with three types of cobalt/molybdenum/aluminum oxide catalyst and with glass spheres. Our aim is also to compare the fit of the different correlations to the present data and to show that predicting correlations relative to water as liquid phase may be somewhat questionable when applied to hydrocarbons.

Experiments were carried out in a 5 cm I.D. column packed to a maximum length of 1.20 m. Properties of the spherical and cylindrical catalyst packings are given in Table 1. This reactor was operated at atmospheric pressure over the range 20° to 30°C. Some results are also taken in a 10 cm I.D. column. Liquid holdup was determined by a weighting method.

When gas and liquid were introduced into the column through flexible P.V.C. tubes, the excess weight over the dry column was weighted by a balance to within 2 g, and liquid holdup was determined after the weight of liquid contained in the entrance and exit tubes was subtracted.

Hydrocarbon liquid properties are presented in Table 2. In the presence of a gas flow rate, kerosene, desulfurized and nondesulfurized gas-oils have a tendency to foam which does not happen with cyclohexane, gasoline, and petroleum ether. However, it was not possible to characterize this by physicochemical parameters such as viscosity, density, and surface tension (see the comparable properties of cyclohexane and kerosene in Table 2). The gas were air, nitrogen, helium, and carbon dioxide ($0.15 < \rho_G < 2$ kg/m³). Superficial mass velocities of 0.5 to 15 kg/m² s and 0 to 1.5 kg/m² s for the liquid and the gas phases, respectively, were used to explore the whole field covered by the various hydrodynamic regimes.

FLOW PATTERNS

Several distinct flow patterns were observed when the liquid flow rate L was kept constant while the gas flow rate G was increased: trickling flow, pulsing flow, and sometimes spray flow for nonfoaming systems and trickling flow (when $G \simeq 0$); foaming flow, foaming pulsing flow, pulsing flow and spray flow for foaming systems. It is very im-

TABLE 2. COEFFICIENTS FOR NONCAPILLARY HOLDUP $\beta_{nc} = AL^a$

	Liquid	β_c	A	a	ρ_L, g/cm³	μ_L, cp	σ_L, dyn/cm
Glass spheres	Water	0.105	0.21	0.37	1	1.1	75
Spherical catalyst	Water	0.11	0.11	0.37	1	1.1	75
Spherical catalyst	Kerosene	0.077	0.26	0.53	0.79	0.99	25.3
Spherical catalyst	Cyclohexane	0.077	0.23	0.46	0.78	0.93	25
Cylindrical catalyst 1	Water	0.08	0.15	0.65	1	1.1	75
Cylindrical catalyst 2	Kerosene	0.077	0.40	0.35	0.79	0.99	25.3
Cylindrical catalyst 2	Cyclohexane	0.077	0.32	0.35	0.78	0.93	25
Cylindrical catalyst 2	Gasoline	0.077	0.31	0.36	0.84	0.57	25.2
Cylindrical catalyst 2	Desulfurized gas-oil	0.08	0.44	0.33	0.86	5	28.8
Cylindrical catalyst 2	Nondesulfurized gas oil	0.08	0.47	0.30	0.86	5	28.3
Cylindrical catalyst 2	Petroleum ether	0.06	0.40	0.40	0.65	0.31	19